



Optics Letters

Maintenance method of signal coherence in lidar and experimental validation

JINGHAN GAO,^{1,2} DAOJING LI,^{1,*} KAI ZHOU,^{1,2} ANJING CUI,^{1,2} JIANG WU,^{1,2} AND YUAN YAO³

¹National Key Laboratory of Science and Technology on Microwave Imaging, Aerospace Information Research Institute, Chinese Academy of Sciences, Beijing, 100190, China

²The School of Electronics, Electrical and Communication Engineering, University of Chinese Academy of Sciences, Beijing, 100049, China

³Changchun Institute of Optics, Fine Mechanics and Physics, Chinese Academy of Sciences, Changchun, Jilin, 130033, China

*Corresponding author: lidj@mail.ie.ac.cn

Received 13 July 2022; revised 30 August 2022; accepted 20 September 2022; posted 20 September 2022; published 11 October 2022

According to the self-heterodyne signal obtained by lidar under different fiber delay times, the model of the local oscillator signal was established, and the maintenance method of signal coherence in lidar based on the digital delay was improved by using multiple sinusoidal frequency modulation components. An imaging detection experiment was carried out at a distance of 5.4 km. The coherence of the lidar signal was maintained by combining the transmitting reference channel correction method and the local oscillator reference channel compensation method, accompanied by the use of a phase spectrum to analyze the improvement effect. The processing results of the echo signal showed that the method could remove the high-order phase errors that cannot be compensated by the phase gradient autofocus algorithm and improve the signal coherence, which could be used for the detection and imaging of long-range targets. © 2022 Optica Publishing Group

<https://doi.org/10.1364/OL.470127>

For lidar with a coherent detection system, due to the instability of the laser signal frequency, the time difference existing between the two signals, i.e., the laser echo signal and the local oscillation signal, will introduce local oscillation phase errors to the mixed signal. Moreover, a greater detection range will result in larger local oscillation (LO) phase errors. Taking inverse synthetic aperture lidar (ISAL) as an example, the azimuth resolution of its imaging results depends on the coherence of the laser signal [1–3], which requires high coherence of the laser signal. It is, therefore, of vital importance to study the maintenance method of the laser signal coherence in the case of long-range action.

The method of local oscillation signal delay is adopted by ISAL to maintain the coherence of the signal [4], with the local oscillation signal delayed by the fiber and then mixed with the echo signal. If the fiber delay time is closer to the time difference between the laser signal from the transmission to reception, the phase errors introduced by the poor frequency stability of the laser signal can be significantly reduced. However, this method is merely applicable to the case where the target range is close and the amount of target range variation is small, instead of being applied in ISAL for long-range target imaging. In Ref. [5],

a method of digitally delaying the LO signal to maintain the coherence of the laser signal is proposed. According to the established laser signal model, the method can estimate the LO phase errors corresponding to the different target ranges and eliminate them. This method can equivalently set different lengths of time-delaying fibers, making the system more flexible and endowed with a large dynamic range, but it requires high accuracy of the laser signal model. On this basis, this paper eliminates the nonlinear phase and random initial phase caused by transmitting high-power signals through the transmitting reference channel and combines the measured data corresponding to different lengths of time-delaying fibers to further improve the laser signal model. The compensation method for the LO phase errors is presented together with relevant experiments being carried out to verify the effectiveness of the coherence maintenance method.

The lidar system used in this paper mainly included a transmitting channel, echo receiving channel, transmitting reference channel (TRC), and LO reference channel (LORC). The reference frequency modulation electrical signal of the acoustic-optic modulator (AOM), the narrow pulse modulation electrical signal of the electro-optic modulator (EOM), and the clock of the analog-to-digital converter (ADC) came from the same crystal oscillator to form a coherent system [6], whose block diagram is shown in Fig. 1. The parameters of the narrow-pulse fiber laser are shown in Table 1, with the linewidth of the LO signal being approximately 1 kHz. A TRC is used to correct the phase errors introduced by high-power transmitting signals [7], and a LORC is adopted to estimate and compensate for the phase errors caused by the frequency instability of the LO signal, both of which are combined to maintain the signal coherence of the lidar.

Ideally, the laser signal should be a single-frequency signal with a stable frequency. In practice, however, the laser oscillates at a single frequency with phase noise, causing a jitter in the frequency domain [8,9]. This paper, therefore, assumes that the center frequency varies sinusoidally. Since the variation of the frequency is affected by the signal generation mechanism, environment, and other factors, it is necessary to use multiple sinusoidal components to characterize it. The laser signal model used in this paper is shown in the following formula:

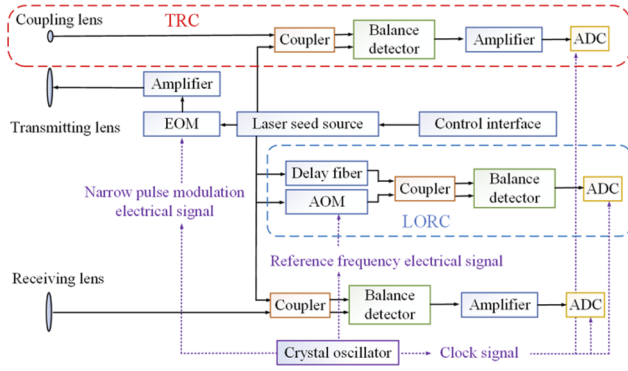


Fig. 1. System block diagram.

Table 1. Parameters of the Narrow-Pulse Fiber Laser

Parameter	Value
Average emitted power	10 W
Pulse width	5 ns
Pulse repetition frequency	100 kHz
Center wavelength	1.55 μm

$$s_{\text{laser}}(t) = \exp\{j2\pi f_c t + \varphi_{\text{sin}}(t) + \varphi_f(t) + \varphi_r(t)\}, \quad (1)$$

where f_c is the center frequency of the laser signal, $\varphi_{\text{sin}}(t) + \varphi_f(t) + \varphi_r(t)$ is the phase errors introduced by the frequency instability of the laser signal, including the phase $\varphi_f(t) = 2\pi \int_0^t f_r(\tau) d\tau$ which is introduced by the random frequency ($f_r(t)$ is the random frequency of the Gaussian distribution), the phase $\varphi_r(t)$ is the random phase of the Gaussian distribution, and the phase $\varphi_{\text{sin}}(t) = 2\pi \sum_{i=1}^N \int_0^t A_{F_i} \sin(2\pi f_{F_i} \tau) d\tau$ which is introduced by the sinusoidal variation of the signal frequency (A_{F_i} is the amplitude of the i th sinusoidal frequency modulation component, f_{F_i} is the i th sinusoidal frequency modulation component).

At present, the main evaluation index of laser signal coherence is the linewidth. A narrower linewidth results in a better signal coherence. Usually, the self-heterodyne technique is adopted to measure the linewidth [10]. Based on the established laser signal model, the low-frequency electrical signal obtained after self-heterodyne could be expressed as

$$s_h(t) = \exp\{j2\pi f_c t_0\} \cdot \exp\{j2\pi f_m t\} \cdot \exp\left\{j2\pi \sum_{i=1}^N \int_{t-t_0}^t A_{F_i} \sin(2\pi f_{F_i} \tau) d\tau\right\} \cdot \exp\left\{j2\pi \int_{t-t_0}^t f_r(\tau) d\tau\right\} \cdot \exp\{j[\varphi_r(t) - \varphi_r(t-t_0)]\}, \quad (2)$$

where f_m is the frequency shift of the AOM and t_0 is the delay time of the optical pulse signal in the fiber.

With the laser emission power kept constant, an optical fiber with lengths of 300 m, 500 m, and 20.5 km was adopted to delay the laser signal and was mixed with the signal output from AOM ($f_m = 100$ MHz). The parameters of the laser model can be determined from the obtained self-heterodyne signal, as shown in Table 2. The comparison between the real signal (RS) and the simulated signal (SS) corresponding to the above fiber lengths is demonstrated in Figs. 2–4. It can be seen from Figs. 2–4 that the simulated signals corresponding to the three fiber lengths are relatively close to the real signals. The basic

Table 2. Parameters in the Laser Model

Parameter	Value	Parameter	Value
A_{F1}	5 kHz	f_{F1}	145 Hz
A_{F2}	2.5 kHz	f_{F2}	270 Hz
A_{F3}	2.5 kHz	f_{F3}	539 Hz
$f_r(t)$	230 kHz	$\varphi_r(t)$	0.01 rad

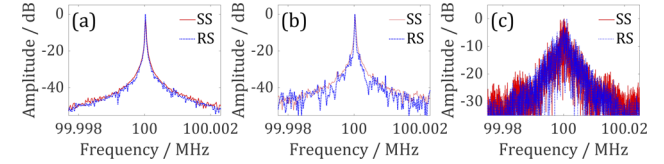


Fig. 2. Spectrum comparison between simulated signal and real signal: (a) 300 m; (b) 500 m; (c) 20,500 m.

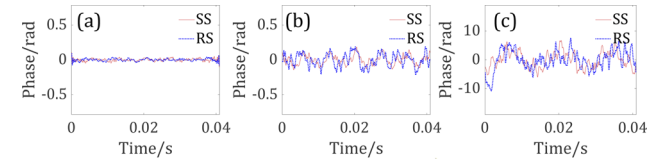


Fig. 3. Phase comparison between simulation signal and real signal after linear phase removal: (a) 300 m; (b) 500 m; (c) 20,500 m.

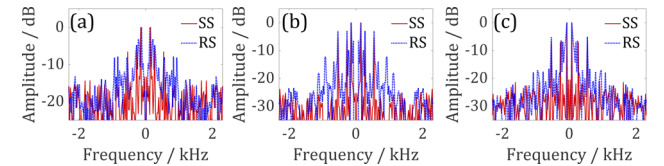


Fig. 4. Phase-spectrum comparison between simulated signal and real signal after linear phase removal: (a) 300 m; (b) 500 m; (c) 20,500 m.

elements of the signal spectrum (center frequency, bandwidth, spurious-frequency components, and noise levels) are the same, the correlation coefficients of the signal spectrum curves are all greater than 0.75, and the correlation coefficients of the phase curves are all greater than 0.32. Additionally, the main peak points in the phase spectrum can also correspond one by one, which indicates that the established laser signal model can be used to simulate real signals.

The linewidth of the LO signal was accurately reflected by the self-heterodyne results of the 20.5-km fiber, with the 3-dB bandwidth of the power spectrum of the self-heterodyne signal being approximately 1.9 kHz, which also confirmed that the linewidth of the laser we used was approximately 1 kHz. The spectrum of the LO signal established according to the model is shown in Fig. 5. Assuming that the frequency of the LO signal is 100 MHz, the single-sideband phase noise $N(f)$ and the corresponding root mean square value $\Delta\phi_{\text{rms}}^2$ of the phase change are shown in Table 3.

In principle, the spectrum of the self-heterodyne signal is equivalent to the Doppler spectrum of the laser echo signal when the ISAL system and the target are relatively stationary. This means that the time coherence between the echo and the LO signal would decrease with the increase of the ISAL detection

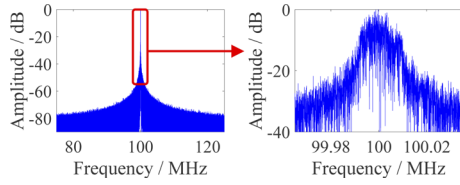


Fig. 5. Spectrum simulation results of LO signal.

Table 3. $N(f)$ and $\Delta\phi_{\text{rms}}^2$

f (kHz)	$N(f)$ *dBc/Hz	$\Delta\phi_{\text{rms}}^2$ (rad)
25	-27	0.089
100	-40	0.014
250	-48	0.006

range, thus affecting the detection range, azimuth resolution, and imaging signal-to-noise ratio (SNR) of the system. The echo signal of a single scattered point can be expressed as

$$\begin{aligned}
 s_d(\hat{t}, t_k) = & \exp\left\{-j4\pi f_c \frac{R(\hat{t}+t_k)}{c}\right\} \cdot \exp\left\{j\varphi_m\left(\hat{t} + t_k - 2\frac{R(\hat{t}+t_k)}{c}\right)\right\} \\
 & \cdot \exp\left\{j\varphi_i\left(\hat{t} + t_k - 2\frac{R(\hat{t}+t_k)}{c}\right)\right\} \\
 & \cdot \exp\left\{j\left[\varphi_{\sin}\left(\hat{t} + t_k - 2\frac{R(\hat{t}+t_k)}{c}\right) - \varphi_{\sin}(\hat{t} + t_k)\right]\right\} \\
 & \cdot \exp\left\{j\left[\varphi_f\left(\hat{t} + t_k - 2\frac{R(\hat{t}+t_k)}{c}\right) - \varphi_f(\hat{t} + t_k)\right]\right\} \\
 & \cdot \exp\left\{j\left[\varphi_r\left(\hat{t} + t_k - 2\frac{R(\hat{t}+t_k)}{c}\right) - \varphi_r(\hat{t} + t_k)\right]\right\}.
 \end{aligned} \quad (3)$$

where \hat{t} is the fast time, t_k is the slow time, $R(\hat{t} + t_k)$ is the distance from the scattering point to the lidar, c is the speed of light, $\varphi_m(\hat{t}, t_k)$ is the phase of the modulated signal, and $\varphi_i(\hat{t}, t_k)$ is the phase errors caused by the transmitted signal.

Laser signals are sensitive to environmental factors such as temperature. In the process of modulation and amplification, nonlinear phases and random initial phases between pulses will be introduced, resulting in nonlinear variation in both the fast-time phase and the slow-time phase of the transmitted signal, which will affect the coherence and imaging performance of echo signals. The time-varying phase of the laser transmitting signal is recorded by the TRC. The matched filter is constructed with the signal from the TRC, and then the echo signal is matched and filtered in the fast-frequency domain to realize phase-error correction.

The phase errors of the transmitted signal during the system working were added to the simulated echo to simulate the point target echo signal. The results before and after the TRC correction are shown in Fig. 6. From the slow-time phase curve and the spectrum of the slow-time phase, the slow-time phase fluctuation of the echo signal after TRC correction was more stable, and part of high-order phase error components was removed. In addition, the 3-dB bandwidth of the Doppler spectrum of the

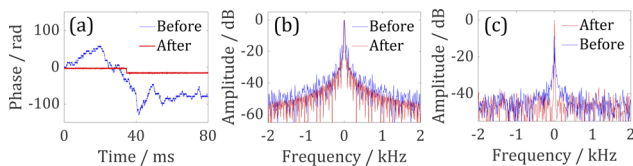


Fig. 6. Comparison of the results before and after using the TRC to correct the echo: (a) slow-time phase; (b) spectrum of slow-time phase; (c) Doppler spectrum.

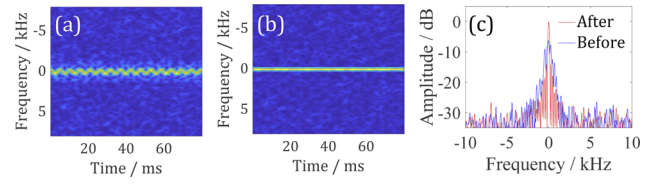


Fig. 7. Comparison of the results before and after using the LORC to correct the echo: (a) time-frequency analysis before compensation; (b) time-frequency analysis after compensation; (c) Doppler spectrum.

echo signal after the correction was narrowed, together with the SNR significantly improved, which indicated the improvement of coherence of the signal.

The only phase errors that can be compensated by the LORC in Eq. (3) were the LO phase errors introduced by the sinusoidal variation of the signal frequency. The simulation generated an echo signal of a point target at a distance of 5 km. The results before and after the LORC compensation are shown in Fig. 7. As can be seen, the LO phase errors were very large, which greatly broadened the 3-dB bandwidth of the Doppler spectrum. Compensating the estimated phase errors into the echo signal in the time domain could improve the coherence of the signal, which is reflected in the following aspects: the center frequency is more stable in the time-frequency analysis results, the 3-dB bandwidth of the Doppler spectrum of the echo signal is narrowed from 781 Hz to 160 Hz, and the signal-to-noise ratio is improved by 6.26 dB.

Here, 8192 pulses of the echo signal are selected for coherent processing, and the results are shown in Fig. 8. The 3-dB bandwidth of the Doppler spectrum of the echo signal before the

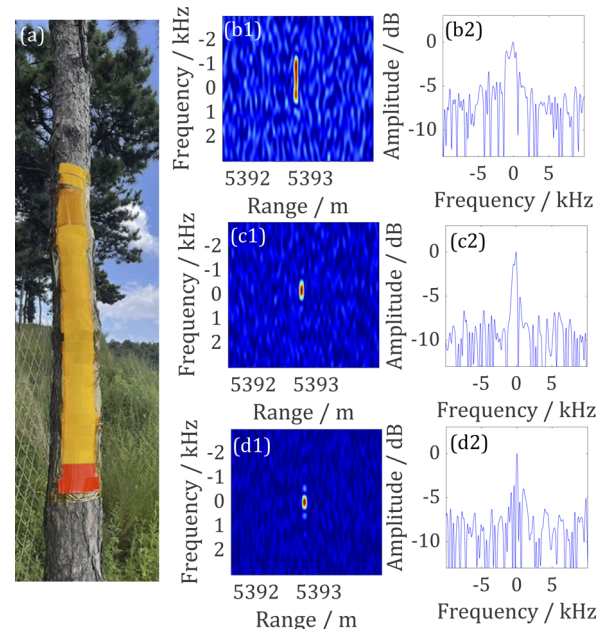


Fig. 8. Correction and compensation effect of TRC and LORC: (a) photo of the target at 5.4 km; (b1) range-Doppler domain imaging results before correction; (c1) range-Doppler domain imaging results after TRC correction; (d1) range-Doppler domain imaging results after TRC correction and LORC compensation. (b2)–(d2) Doppler spectrum profile of panels (b1)–(d1) at the range corresponding to the target.

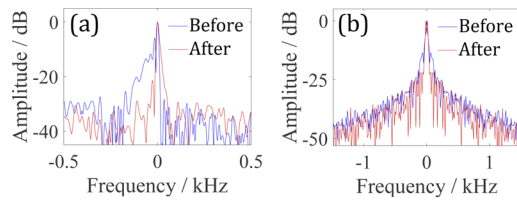


Fig. 9. Comparison of echo processing results with PGA processing before and after correction and compensation: (a) Doppler spectrum; (b) spectrum of slow-time phase.

correction was approximately 1.660 kHz., which was reduced to 293 Hz after the TRC correction; meanwhile, the SNR was improved by approximately 3 dB. By compensating the LO phase errors corresponding to 5.4 km, the 3-dB bandwidth of the Doppler spectrum can be further reduced to 74 Hz.

The above method could effectively improve the coherence of the signal and significantly improve the Doppler frequency resolution of ISAL, while it did not decrease the 3-dB bandwidth of the Doppler spectrum to 12 Hz (corresponding to the coherent processing time), which was caused by the inability of the proposed method to compensate for the random phase (only a small part) as well as the phase errors caused by atmospheric turbulence, resulting in the sidelobe still at a high level. These phase errors could be further processed by the phase gradient autofocus (PGA) algorithm [11]. The results of PGA processing on the echo signals before and after correction and compensation are shown in Fig. 9. The results show that after PGA processing, the 3-dB bandwidth of the Doppler spectrum was reduced from 74 Hz to 14 Hz, close to the ideal 12-Hz frequency resolution.

However, the PGA algorithm could only compensate for the low-order phase errors, and was invalid for the high-order phase errors. If the echo is directly processed with the PGA algorithm, it would always be affected by high-order phase errors, and as a result, the focusing effect would be reduced and the ideal resolution would be difficult to obtain, which is also reflected in Fig. 9. Compared with the result of direct PGA processing without

correction and compensation, using the method proposed in this paper, before PGA processing was better to obtain a better focusing effect and a narrower 3-dB bandwidth of the Doppler spectrum. It can be seen from Fig. 9(b) that when the PGA processing was performed after the TRC correction and LORC compensation, compared with the case when the PGA processing was performed directly, the spectrum of the slow-time phase had fewer frequency components, which showed that the method proposed in this work could remove the high-order phase errors that cannot be compensated by PGA processing, and a better focusing effect can be obtained after PGA processing was performed after the TRC correction and the LORC compensation.

Funding. Key deployment projects of Chinese Academy of Sciences (E03701010F).

Disclosures. The authors declare no conflicts of interest.

Data availability. Data underlying the results presented in this paper are not publicly available at this time but may be obtained from the authors upon reasonable request.

REFERENCES

1. S. M. Beck, J. R. Buck, and W. F. Buell, *Appl. Opt.* **44**, 7621 (2005).
2. M. Bashkansky, R. L. Lucke, and E. Funk, *Opt. Lett.* **27**, 1983 (2002).
3. D. Liu, E. Dai, and X. Nan, *Proc. SPIE* **7442**, 744214 (2009).
4. A. B. Gschwendtner and W. E. Keicher, *Lincoln Laboratory J.* **12**, 383 (2000).
5. X. Hu, D. Li, and X. Zhao, *Chin. J. Lasers* **45**, 510003 (2018).
6. D. Li, K. Zhou, and A. Cui, *Laser Optoelectron. Progress* **58**, 1811017 (2021).
7. A. Cui, D. Li, and J. Wu, *Appl. Opt.* **61**, 5466 (2022).
8. Q. Zhou, J. Qin, and W. Xie, *Opt. Express* **23**, 29245 (2015).
9. T. Hidemi, *Opt. Lett.* **36**, 681 (2011).
10. E. Fomiryakov, D. Kharasov, S. Nikitin, O. Nanii, and V. Treshchikov, *J. Lightwave Technol.* **39**, 5191 (2021).
11. D. E. Wahl and P. H. Eichel, *IEEE Trans. Aerosp. Electron. Syst.* **30**, 827 (1994).